acta physica slovaca vol. 45 No. 6, 633 – 644 December 1995

PREEQUILIBRIUM MODEL FOR PHOTONUCLEAR REACTIONS UP TO THE PION THRESHOLD[1]

M.B. Chadwick[2]
University of California, Nuclear Data Group,
Lawrence Livermore National Laboratory, Livermore, CA 94550, USA

P.G. Young[3]
University of California, Theoretical Division,
Los Alamos National Laboratory, Los Alamos, NM 87545, USA

Received 23 October 1995, accepted 27 October 1995

We describe a photonuclear reaction theory for photons with incident energies up to 140 MeV. Photoabsorption is modeled through the giant resonance at the lower energies, and the quasideuteron (QD) mechanism at higher energies. After the initial interaction, primary and multiple preequilibrium emission of fast particles can occur, followed by sequential Hauser-Feshbach decay. Preequilibrium decay is calculated with an exciton model, based on a $2p1h$ initial state to approximate correlation effects in the QD mechanism, as proposed by Blann. A theory for photonuclear angular distributions is given, based on momentum conservation considerations, allowing the calculation of double-differential emission spectra. We compare our calculated angular distribution predictions with measurements for reactions on carbon, and obtain satisfactory agreement. The low momentum of a photon compared to a nucleon projectile of the same energy results in QD photonuclear angular distributions being less forward-peaked than their nucleon counterparts. Theoretical predictions of photonuclear reactions on lead are also compared with data. The theory is able to account for measured excitation functions of neutron emission reactions, along with neutron emission multiplicities.

1. Introduction

A model of photonuclear reactions must account for a number of different nuclear reaction mechanisms involved in the initial photonuclear excitation process, and the subsequent decay of the excited nucleus by particle emission. At low energies, below

[1] Presented at the International Symposium on Pre-Equilibrium Reactions, Smolenice Castle, 23 – 27 October, 1995

[2] E-mail address: CHADWICK@PD4.LLNL.GOV
[3] E-mail address: PGY@LANL.GOV

0323-0465/95

about 30 MeV, the Giant-Dipole Resonance (GDR) is the dominant excitation mechanism, where a collective bulk oscillation of the neutrons against the protons occurs. At higher energies, where the wavelength of the photon decreases, photoabsorption on a neutron-proton (quasi-deuteron (QD)) becomes important. In these processes, the initial nuclear excitation can be described by particle-hole excitations ($1p1h$ for the GDR; $2p2h$ or $2p1h$, as we discuss later, for QD processes) and thus it is natural to use a preequilibrium theory to describe the processes of preequilibrium emission, and damping to equilibrium, during the evolution of the reaction. The present work can be used to calculate photonuclear reactions for incident photons with energies below 140 MeV, which is the threshold for pion production.

Two previous works in particular have demonstrated the usefulness of semiclassical preequilibrium models in describing photonuclear reactions: Wu and Chang's work [1] on an exciton model; and Blann's studies [2] using the hybrid model; both of which utilize a Weisskopf-Ewing evaporation theory to describe the subsequent equilibrium decay. Our work here, which describes new capabilities recently built into the GNASH modeling code [3], makes use of many of the ideas from these papers, but with the following new features: (1) We present a theory for calculating photonuclear angular distributions, enabling a determination of the double-differential cross sections of ejectiles; (2) Full angular momentum and parity conservation is included in a Hauser-Feshbach treatment of equilibrium emission, accounting for the fact that an E1-photon brings in one unit of angular momentum; (3) The initial photoabsorption cross section in the QD regime can be obtained from the theory of Ref. [4]; (4) We include a description of multiple-preequilibrium emission processes which become important when the photon energy exceeds about 50 MeV.

In addition to basic physics interests, applications where photonuclear reactions are important have stimulated this work. In medical accelerators producing bremsstrahlung photons for radiotherapy, the production of photoneutrons in the accelerator structural materials (the beam pipe, collimators, beam modifiers, *etc.*) needs to be understood for radiation protection and dosimetry considerations. Also, photons with energies as high as 50 MeV produced in a fusion reactor can undergo photonuclear reactions, producing high-energy neutrons.

In Sec. 2 we describe the theories used for photoabsorption. Sec. 3 gives some examples of the application of the theory to photonuclear reactions on lead and carbon, making comparisons with experimental data, and our conclusions are given in Sec. 4.

2. Theory

2.1. The Photoabsorption Model

If experimental data exists for the total photoabsorption cross section, it can be used in GNASH calculations via an input file. The most useful type of experimental data here are from photon absorption experiments which really measure the total photoabsorption cross section. For heavy nuclei, compilations of photoneutron total cross section such as that of Dietrich and Berman [5] can be used to approximate the photoabsorption cross

sections, since contributions from photoproton reactions (and other reactions producing complex charged particles) are suppressed by the Coulomb barrier. However, in light nuclei this approach cannot be used since the photoproton cross section is no longer small, and in some cases exceeds the photoneutron cross section. In such cases one should rely only on absorption-type data.

An alternative way to obtain the photoabsorption cross section is from a model [4],

$$\sigma_{abs}(\epsilon_\gamma) = \sigma_{GDR}(\epsilon_\gamma) + \sigma_{QD}(\epsilon_\gamma) \quad (1)$$

in which $\sigma_{GDR}(\epsilon_\gamma)$ is given by a Lorentzian shape, with parameters describing the total absorption of the GDR, and $\sigma_{QD}(\epsilon_\gamma)$ is taken from the QD theory of theory of Ref. [4], which uses a Levinger-type theory to relate the nuclear photoabsorption cross section to the experimental deuteron photodisintegration cross section $\sigma_d(\epsilon_\gamma)$,

$$\sigma_{QD}(\epsilon_\gamma) = L\,\frac{NZ}{A}\,\sigma_d(\epsilon_\gamma)\,f(\epsilon_\gamma) \quad (2)$$

where the Levinger parameter was derived to be $L = 6.5$, and $f(\epsilon_\gamma)$ is the Pauli-blocking function, which reduces the free deuteron cross section $\sigma_d(\epsilon_\gamma)$ to account for Pauli-blocking of the excited neutron and proton by the nuclear medium. The experimental deuteron photodisintegration cross section was parameterized as $\sigma_d(\epsilon_\gamma) = 61.2(\epsilon_\gamma - 2.224)^{3/2}/\epsilon_\gamma^3$ mb. The Pauli-blocking was derived by Chadwick *et al.* to be a multidimensional integral whose solution could be well approximated in the energy range $20 - 140$ MeV by the polynomial expression

$$f(\epsilon_\gamma) = 8.3714\times10^{-2} - 9.8343\times10^{-3}\epsilon_\gamma + 4.1222\times10^{-4}\epsilon_\gamma^2 - 3.4762\times10^{-6}\epsilon_\gamma^3 + 9.3537\times10^{-9}\epsilon_\gamma^4. \quad (3)$$

In Ref. [4] the Pauli-blocking function was not parameterized below 20 MeV, where it tends to zero, or above 140 MeV, where it tends to unity. Still, as the contribution needs to be defined at all energies considered, we use an exponential shape $f(\epsilon_\gamma) = \exp(-D/\epsilon_\gamma)$ for energies below 20 MeV, and above 140 MeV, with $D = -73.3$ for $\epsilon_\gamma < 20$ MeV and $D = 24.2$ for $\epsilon_\gamma > 140$ MeV. This form has the correct behavior in that it tends to zero at $\epsilon_\gamma = 0$, and unity for large ϵ_γ and is continuous with Eq. (3) at 20 and 140 MeV.

2.2. Preequilibrium Exciton Model

Particle and hole excitations are produced in the nucleus following photoabsorption. Particle emission can occur from such a state yielding the typically high-energy preequilibrium emission; or alternatively, a nucleon-nucleon interaction may occur producing more particle-hole excitations. The composite nuclear system passes through such stages of increasing complexity towards equilibrium, and the total preequilibrium emission is the sum of contributions from all the preequilibrium stages.

Wu and Change [1] and Blann [2] have successfully applied preequilibrium physics modeling to describe the emission of high-energy nucleons following photoabsorption.

Wu and Chang used an initial $2p2h$ state in the preequilibrium cascade, while Blann argued that the two holes are correlated through the QD mechanism, and therefore can be approximately treated as one degree of freedom, i.e. a $2p1h$ initial state. We follow Blann's prescription, and use the Kalbach exciton model in GNASH [3] to calculate the preequilibrium emission of fast nucleons. Once the incident photon energy exceeds about 50 MeV, multiple preequilibrium emission (MPE) becomes important, where more than one fast particle is emitted. For this we use the generalized MPE model of Ref. [6]. For both primary and multiple preequilibrium emission, we modified the neutron-proton distinguishability factors to reflect the initial particle-hole type appropriate for the QD mechanism (i.e. of the two particles, one is a neutron and the other a proton).

As in nucleon-induced reactions, we expect the angular distribution of preequilibrium nucleons to be forward-peaked since the incident projectile's energy and momentum are shared among the particle and hole degrees of freedom, and momentum conservation leads to a higher probability of emission in the forward direction. But since the momentum of a photon is considerably smaller than that of a nucleon for the same energy, the degree of forward peaking will be smaller for photonuclear reactions. Chadwick and Oblozinsky [7] recently derived a theory for continuum angular distributions which provides a physical basis for the Kalbach angular-distribution systematics. This theory, which uses state densities with linear momentum to obtain preequilibrium angular distributions, can be applied to obtain the angular distributions of the fast particles. From the preequilibrium stage characterized by n excitons the angular distribution is given by an exponential in $\cos\theta$,

$$G(n,\theta) = \frac{1}{4\pi}\frac{2a}{e^a - e^{-a}}\exp(a\cos\theta). \qquad (4)$$

The a-parameter governs the degree of forward peaking and is given by

$$a = \frac{3Kk_\Omega}{2n_r m\epsilon_{\rm av}}, \qquad (5)$$

where K is the incident photon momentum, k_Ω is the emitted nucleon momentum relative to the bottom of the nuclear well, n_r is the number of excitons in the residual nucleus (since we adopt Blann's prescription of using a $2p1h$ initial state, n_r=2 for 1st-stage emission, *etc*), and m is the nucleon mass. $\epsilon_{\rm av}$ is the average exciton energy relative to the bottom of the well as given in Ref. [7].

The above formulation enables angular distributions in preequilibrium reactions to be determined straightforwardly. As discussed in detail in Ref. [7], its derivation incorporates full momentum conservation for all orders of scattering, and does not make a leading-particle approximation. Additionally, in the non-statistical limit there are close links with the Kikuchi-Kawai approach (often used for nucleon reactions) as discussed in Refs. [7, 8]. In this work we do not concentrate on the angular distribution of particles emitted at low energies. Experimental data for such emission frequently exhibits a dipole distribution, peaked at 90-degrees, due to the dominant E1-contribution. However, the angular variation is strongly dependent on the reaction mechanism involved, with direct processes often exhibiting a dipole shape and evaporative contributions in heavy nuclei exhibiting isotropy.

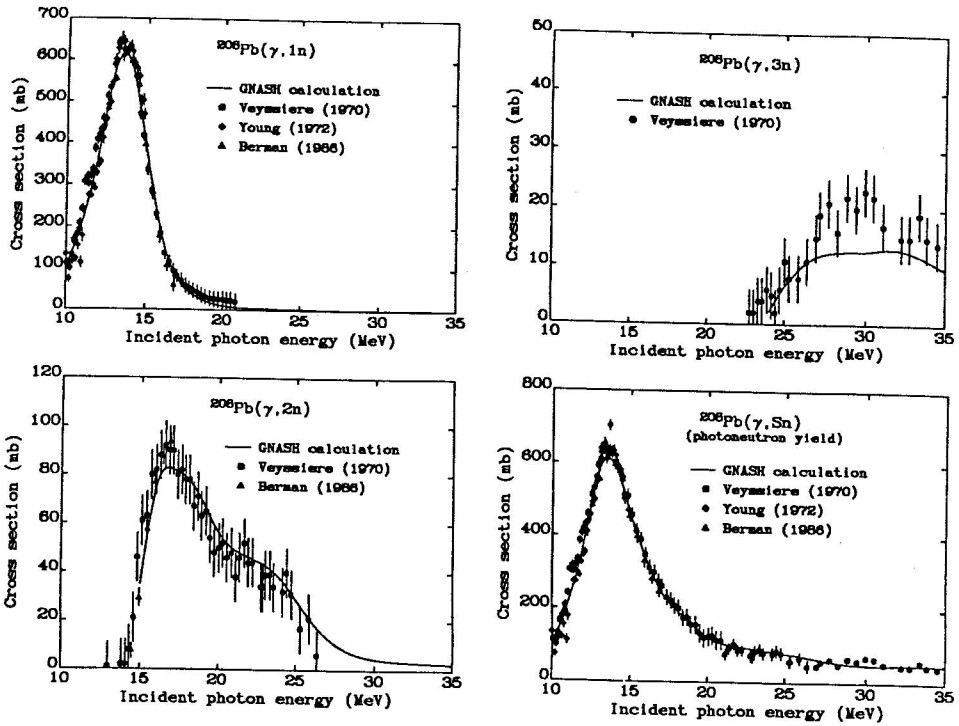

Fig. 1. Measured ^{208}Pb+γ photoneutron yield, and photoneutron excitation functions, compared with model calculations.

3. Results

To test our photonuclear modeling we study reactions on two different nuclei: lead and carbon. These two nuclei were chosen since they illustrate different features that must be addressed in modeling photonuclear reactions, and a significant amount of experimental data exists for them. For lead there are data for excitation functions of multiple-neutron emission which allow a test of our work. Carbon, on the other hand, is one of the very few nuclei for which double-differential photoneutron and photoproton spectra exist, from monoenergetic photons, allowing a direct test of our calculated QD angular distributions. We describe our results for these two cases below.

3.1. γ+ ^{208}Pb

In our calculations we use the optical model and level density parameters described in Ref. [9]. The total photonuclear absorption cross section was first evaluated from the existing data. We compare our model calculations for lead with experimental data measured at Saclay, Illinois, and Livermore.

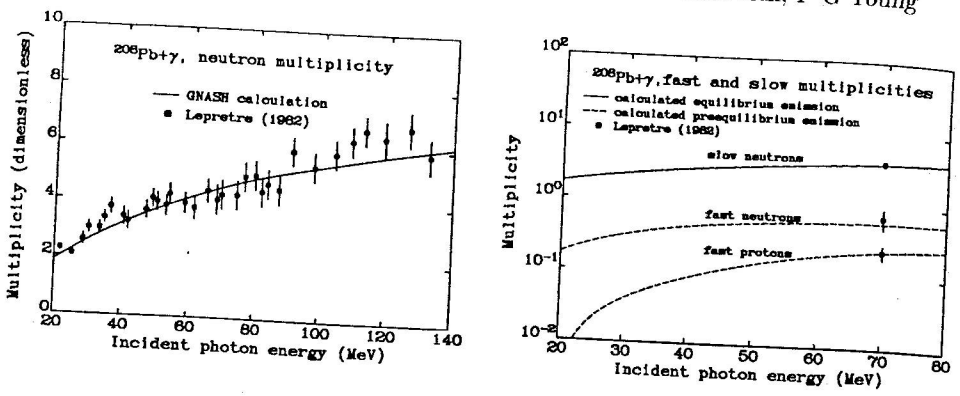

Fig. 2. Measured ^{208}Pb+γ particle emission multiplicities, compared with model calculations. See text for discussion.

For the lower photon energies, experimental measurements are summarized in the Livermore compilation of Dietrich and Berman [5]. In a later work, Berman *et al.* concluded [10] that the earlier Livermore measurements on lead were too low, and therefore we do not include the early Livermore measurements [11]. In Fig. 1 we show measurements [10, 12, 13] of the ^{208}Pb(γ,1n), ^{208}Pb(γ,2n), ^{208}Pb(γ,3n), excitation functions and the photoneutron yield cross section, compared with our calculations. Our calculations are seen to describe the measurements well.

In Fig. 2 we show our calculated multiplicities for particle emission compared with the measurements of Lepretre *et al.* [14]. The left-hand figure shows the average neutron multiplicity, which is well described by our calculations. The right-hand figure shows the measured fast and slow multiplicities at an incident photon energy of 70 MeV, compared with our calculations. The fast multiplicity refers to the preequilibrium particles, while the slow multiplicity refers to the compound nucleus particles, and our calculations are seen to describe the correct partitioning of ejectiles among preequilibrium and equilibrium emission, and between neutrons and protons. These measurements are invaluable for testing the preequilibrium modeling in our calculation, since direct measurements of the nucleon emission spectra from monoenergetic photons do not exist for lead. The large Coulomb barrier in lead is responsible for the excess of fast preequilibrium neutrons compared to protons; at the highest energies the differences are reduced. In general the slow neutron multiplicity is much larger than the fast multiplicities, since preequilibrium decay accounts for at most the first two emissions, with the subsequent sequential particle decays coming from compound-nucleus emission. There is a nice discussion in Lepretre's paper [14] commenting on the slope of the average neutron multiplicity curve, which is worth repeating: If preequilibrium emission did not occur, each emitted neutron would require approximately 10 MeV (separation energy plus evaporation kinetic energy), and so the multiplicity curve would increase with a slope of 1 unit for every 10 MeV incident energy. The data in Fig. 2 show such a steep slope at the lowest incident energies, but for higher energies a much smaller slope

occurs due to the higher kinetic energy carried by preequilibrium ejectiles.

Other data also exist for lead which we do not show here (we have presented our calculations compared with these data in Ref. [15]). Lepretre *et al.* [16] obtained excitation functions for ^{208}Pb(γ,xn) reactions (x=1–12), for incident photon energies up to 140 MeV, and our calculations described them well [15]. Also, while photoneutron emission spectra from mono-energetic photons on lead do not exist, a measurement of the photoneutron spectrum at 67 degrees from bremsstrahlung photons was made at Rensselaer Polytechnic Institute by Kaushal *et al.* [17]. This measurement was made by subtracting photoneutron spectra resulting from two separate beams: a bremsstrahlung beam with maximum energy of 85 MeV; and a bremsstrahlung beam with maximum energy of 55 MeV. The resulting neutron "difference spectrum" is due to photon incident energies between 55 and 85 MeV, and there is good agreement with our calculation [15].

3.2. γ+ ^{12}C

We study carbon primarily because our preequilibrium angular distribution theory can be tested – more photonuclear experimental data exists for carbon than for probably any other nucleus, and it is one of the very few cases where monochromatic photonuclear double-differential spectra exist. The above statistical theory cannot be immediately applied in the analysis of photonuclear reactions on carbon, since there are significant contributions from direct reactions. In particular the (γ, n_0) and (γ, p_0) processes, which result in the residual nucleus being left in its ground state, account for a significant fraction of the photonuclear cross section (particularly for low incident energies). Therefore we first evaluate the ^{12}C(γ, n_0) and the ^{12}C(γ, p_0) cross sections from the available experimental data. These pre-evaluated direct cross sections are then subtracted from the evaluated photoabsorption cross section, and the remaining cross section is used as an input in the GNASH preequilibrium and equilibrium calculations. Before comparing our results for double differential photoproton data, we first review the many previous works on carbon which have elucidated the nuclear reaction mechanism.

Results from previous analyses. The near equality of the (γ,p) and (γ,n) cross sections [18, 19, 20] suggests an initial interaction with a correlated neutron-proton pair, i.e a quasideuteron. QD calculations of McGeorge [20], using a model similar to that of Schier and Schoch [19], provided a reasonably good description of the photoproton spectra at 60 and 80 MeV, except for the photoprotons at the highest energies where a quasifree-knockout model provided a somewhat better description of the data. Calculations by Ireland *et al.* [21] also showed that a QD model can reasonable predict the photoproton spectra except at the highest proton energies. The highest photoproton energy transitions were poorly described by both a QD model and a knockout model. Generally, theoretical models are unable to account for the (γ, p_0) cross sections at incident energies above 50 MeV.

Fuller based his 1985 evaluation [22] of the (γ, p_0) cross section up to 30 MeV on the data of Allas *et al.* [23] (obtained by detailed balance from (p, γ_0) measurements) up to 29 MeV, supplemented by the data of Snover *et al.* [24] up to 30 MeV. More recent measurements of this cross section by Kerkhove *et al.* [25] agree well with Allas

et al.'s results. The data of Carchon *et al.* [26] was not included since no attempt was made to separate the ground-state from excited state transitions. Also, the results of Allas *et al.* and Kerkhove *et al.* indicate that the Collins *et al.* [27] measurement is too low. Fuller's result for the Allas *et al.* (γ,p_0) cross section at the peak of the GDR (22.5 MeV) of 11 ± 1.1 mb is in excellent agreement with Kerkhove *et al.*'s [25] value of 11.0 ± 1.1 mb. There is some ambiguity concerning the ratio of (γ,p_i) to excited states to (γ,p_0) at 28 MeV; Fuller's evaluation for the total photoproton cross section was based on a subtraction of the measured photoneutron, alpha, and ^{3}He from the total photoabsorption cross section, and resulted in a ratio of 0.49 compared to Ferdinande *et al.*'s 0.24 [28].

At higher incident photon energies, a number of experiments have measured photoproton cross sections from monoenergetic photons. At 60, 80, and 100 MeV, experimental values for the total (γ,p_0) cross section have been tabulated by Matthews *et al.* [18], after angle-integrating their differential data. These measurements have been subsequently confirmed by numerous other papers: differential cross section measurements to the ground and excited states of ^{11}B have been made by Springham *et al.* [29] (49-78.5 MeV), Shotter *et al* [30] (60 MeV), McGeorge *et al.* [20] (60 and 80 MeV), and Ireland *et al.* [21] (60 MeV). For photons with incident energies above about 50 MeV these experiments show a strongly forward-peaked angular distribution for the (γ,p_0) cross section (for example, the ratio of the cross section at 60 and 120 degrees, at 60 MeV, is about 10:1) [29, 20, 30]. However, transitions to the excited states typically are far less forward-peaked, showing an analogous ratio at 60 MeV of approximately 2:1 [20, 29, 30].

Fuller evaluated the (γ,n) based on the measurements of Wu *et al.* [31]. Harty *et al.* [32] measured (γ,n) cross sections to the ground state and excited states at 65 degrees, for energies between 30 and 100 MeV. These are in good agreement with the results of Schier and Schock, who measured (γ,n) [19] in the 60-150 MeV range, and (γ,n_0) [33] at 60 MeV. They noted that the cross sections for (γ,n) and (γ,p) processes are comparable in magnitude, and both show a forward asymmetry in the angular distributions. They conclude that two-body effects are important, and model the reaction in terms of a QD model (except for ground-state transitions), and also a microscopic model which includes meson exchange currents. These calculations lead to a good description of the (γ,n_0) cross sections. Below 30 MeV Fuller evaluated the (γ,n_0) cross section based on the measurements of Fultz *et al.* [34] (multiplied by 1.17, to be consistent with other measurements – with this renormalization, the data is consistent with that by Lochstet *et al.* [35] and Kneissl *et al.* [36]). There is also data by Cook [37] for the ^{12}C$(\gamma,1n)^{11}$C.

Calculated double-differential spectra compared to data. The experimental data and evaluations noted in the above section allowed us to evaluated the carbon total photoabsorption cross section (which we based on Ahren's data [38]), and the direct (γ,n_0) and (γ,p_0) cross sections. Following this, we used our photonuclear model in the GNASH code to calculate photoproton emission spectra at 60 and 80 MeV, for comparison with the McGeorge *et al.* monochromatic double-differential data. This allows a test of our angular distribution theory (Eqs. 4,5).

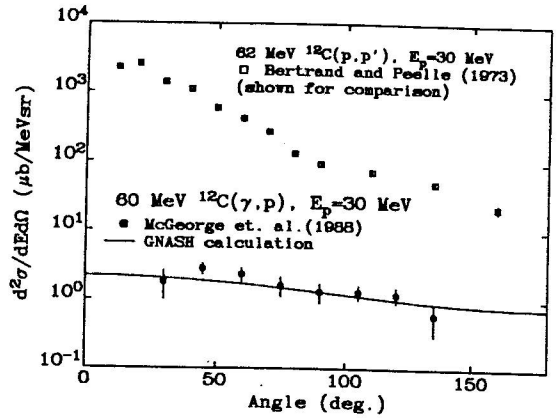

Fig. 3. Calculated angular distribution for the 60 MeV ^{12}C(γ,p') reaction, for protons with an emission energy of 30 MeV, compared with measurements of McGeorge et al. (1986). For comparison, we show experimental data measured by Bertrand and Peelle (1973) for the *proton*-induced reaction ^{12}C(p,p'), which are seen to be far more forward-peaked.

In Fig. 3 we compare the calculated angular distribution with experimental data for 60 MeV incident photons, for protons emitted at 30 MeV. It is evident that the calculation agrees with the data fairly well, predicting a small amount of forward-peaking. For comparison, we show the angular distribution data measured by Bertrand and Peelle [39] in the equivalent *proton*-induced reaction, which is much more forward-peaked. As explained by our theory, the reduced forward-peaking for QD photonuclear reactions is due to the small momentum carried by a photon.

Figure 4 shows our calculated 80 MeV proton emission spectra at a range of angles compared with data. Again, the calculated photoproton emission spectra describe the measurements well. The structure seen in the calculations, and in the data, at high energies is due to the presence of discrete states at low residual-nucleus excitation energies. Fig. 4 also shows a calculation where the angular variation, instead of being obtained theoretically using Eqs. (4,5) is determined with a phenomenological "systematics" formula we presented in Ref. [40]. The systematics approach is more suitable for applications, since double differential spectra are determined from the angle-integrated spectra immediately without including different angular distributions from each preequilibrium stage. While the use of our systematics also gives results which agree well with the data, that approach is not grounded in a physical derivation to the same extent as the present work.

4. Conclusions

We have shown that this photonuclear model describes the available experimental data up to photon energies of 140 MeV. The preequilibrium modeling, using a QD mechanism, was tested indirectly for reactions on lead by studying multiplicities and photoneutron excitation functions. In the case of carbon, the preequilibrium emission

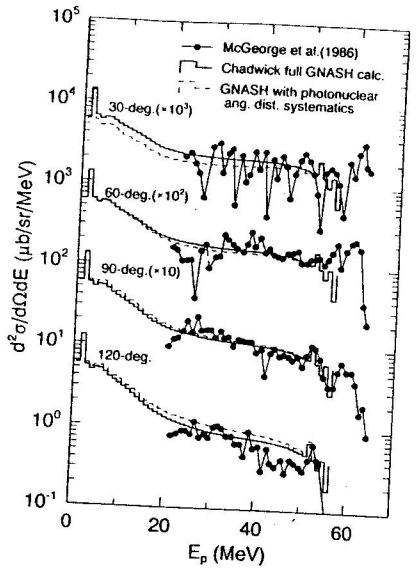

Fig. 4. Calculated emission spectra, at various angles, for the 80 MeV $^{12}C(\gamma,p')$ reaction, compared with measurements of McGeorge et al. (1986). Also shown are calculated results using the photonuclear systematics of Ref. [40].

model (including our angular distribution theory) was tested directly by comparing calculations of double-differential photoproton spectra with measurements. Our theoretical prediction that QD photonuclear angular distributions are less forward peaked than those for nucleon reactions is supported by the measurements. Interestingly, while our angular distribution theory [7] for nucleon-induced reactions underestimated backangle emission below 80 MeV, this theory applied to photon reactions appears to work well. This is, presumably, because diffraction and refraction effects which are important in nucleon induced reactions are less important for a photon projectile, since they are not present in the incident channel.

Acknowledgments We thank M. Blann for his comments on the approaches that can be used for modeling photon induced reactions, and S. Warshaw and N. Chakravarty for useful discussions. This work was performed under the auspices of the U.S. Department of Energy by Lawrence Livermore National Laboratory under contract No. W-7405-Eng-48, and by Los Alamos National Laboratory under contract No. W-7405-Eng-36.

References

[1] J.R. Wu, C.C. Chang: *Phys. Rev. C* **16** (1977) 1812
[2] M. Blann, B.L. Berman, T.T. Komoto: *Phys. Rev. C* **28** (1983) 2286
[3] P.G. Young, E.D. Arthur, M.B. Chadwick: Los Alamos National Laboratory report LA-MS-12343 (1992)

[4] M. B. Chadwick, P. Oblozinsky, G. Reffo, P.E. Hodgson: *Phys. Rev. C* **44** (1991) 814
[5] S.S. Dietrich, B.L. Berman: *Atomic Data and Nuclear Data Tables* **38** (1988) 199
[6] M.B. Chadwick, P.G. Young, D.C. George, Y. Watanabe: *Phys. Rev. C* **50** (1994) 996
[7] M.B. Chadwick, P. Oblozinsky: *Phys. Rev. C* **50** (1994) 2490
[8] M.B. Chadwick, P. Oblozinsky: *Phys. Rev. C* **46** (1992) 2028
[9] P.G. Young, M.B. Chadwick: *in* Specialist Meeting on Intermediate Energy Nuclear Data. *Issy-les-Moulineaux 1994 (Ed. P. Nagel).* NEA?OECD 1994, p. 49;
H. Vonach, A. Pavlik, M.B. Chadwick, R. Haight, R. Nelson, P.G. Young: *Phys. Rev. C* **50** (1994) 1952
[10] B.L. Berman et. al.: *Phys. Rev. C* **36** (1987) 1286
[11] R.L. Bramblett, J.T. Caldwell, B.L. Berman, R.R. Harvey, S.C. Fultz: *Phys. Rev.* **148** (1966) 1198
[12] A. Veyssiere, H. Beil, R. Bergere, P. Carlos, A. Lepretre: *Nucl. Phys.* **A159** (1970) 561
[13] L. M. Young: Ph.D. thesis, University of Illinois, (1972)
[14] A. Lepretre, H. Beil, R. Bergere, P. Carlos, J. Fagot, A. Veyssiere, I. Halpern: *Nucl. Phys. A* **390** (1982) 221
[15] M.B. Chadwick, P.G. Young: Lawrence Livermore National Laboratory report UCRL-ID-118721 (1994)
[16] A. Lepretre, H. Beil, R. Bergere, P. Carlos, J. Fagot, A. de Miniac, A. Veyssiere: *Nucl. Phys. A* **367** (1981) 237
[17] N. Kaushal *et al.*: *Phys. Rev.* **175** (1986) 1330
[18] J.L. Matthews, D.J.S. Findlay, S.N. Gardiner, R.O. Owens: *Nucl. Phys. A* **267** (1976) 51
[19] H. Schier, B. Schoch: *Nucl. Phys. A* **229** (1974) 93
[20] J.C. McGeorge, G.I. Crawford, R.O. Owens, M.R. Sene, D. Branford, A.C. Shotter, B. Schoch, R. Beck, P. Jennewein, F. Klein, J. Vogt, F. Zettl: *Physics Lett. B* **179** (1986) 212
[21] D.J. Ireland, D. Branford, T. Davinson, N.J. Davis, E.W. Macdonald, P.J. Sellin, A.C. Shotter, P. Terzoudi, P.J. Woods, J.O. Adler, B.E. Anderson, L. Isaksson, D. Nilsson, H. Ruijter, A. Sandell, B. Schroder: *Nucl. Phys. A* **554** (1993) 173
[22] E.G. Fuller: *Phys. Rep.* **127** (1985) 185
[23] R.G. Allas, S.S. Hanna, L. Meyer-Schutzmeister, R.E. Segel: *Nucl. Phys.* **58** (1964) 122
[24] K.A. Snover, P. Paul, H.M. Kuan: *Nucl. Phys. A* **285** (1977) 189
[25] E. Kerkhove, P. Berkvens, R. Van de Vyver, D. Ryckbosch, P. Van Otten, H. Ferdinande, E. Van Camp, A. De Graeve: *Phys. Rev. C* **33** (1986) 1796
[26] R. Carchon, R. Van de Vyver, H. Ferdinande, J. Devos, E. Van Camp: *Phys. Rev. C* **14** (1976) 456
[27] M.T. Collins, S. Manglos, N.R. Roberson, A.M. Sandorfi, H. R. Weller: *Phys. Rev. C* **26** (1982) 332
[28] H. Ferdinande, D. Ryckbosch, E. Kerkhove, P. Berkvens, R. Van de Vyver, A. De Graeve, L. Van Hoorebeke: *Phys. Rev. C* **39** (1989) 253
[29] S.V. Springham, D. Branford, T. Davinson, A.C. Schotter, J. Yorkston, J. C. McGeorge, J.D. Kellie, S.J. Hall, R. Beck, P. Jennewein, B.Schoch: *Nucl. Phys. A* **517** (1990) 93
[30] A.C. Shotter, S. Springham, D. Branford, J. Yorkston, J.C. McGeorge, B. Schoch, P. Jennewein: *Phys. Rev. C* **37** (1988) 1354

[31] C.P. Wu, F.W.K. Firk, T.W. Phillips: *Phys. Rev. Lett.* **20** (1968) 1182

[32] P.D. Harty, M.N. Thompson, G.J. O'Keefe, R.P. Rassool, K. Mori, Y. Fujii, T. Suda, I. Nomura, O. Konno, T. Teresawa, Y. Torizuka: *Phys. Rev. C* **37** (1988) 13

[33] H. Schier, B. Schoch: *Lett. Nuovo Cim.* **12** (1975) 334

[34] S.C. Fultz: *Phys. Rev. C* **143** (1966) 790

[35] W.A. Lochstet, W.E. Stephens: *Phys. Rev.* **141** (1966) 1002

[36] U. Kneissl, E.A. Koop, G. Kuhl, K.H. Leister, A. Weller: *Nucl. Instr. Meth.* **127** (1975) 1

[37] B.C. Cook, J.E.E. Baglin, J.N. Bradford, J.E. Griffin: *Phys. Rev.* **143** (1966) 724

[38] J. Ahrens, H. Borchert, K.H. Czock, H.B. Eppler, H. Gundrum, M. Kroning, P. Riehn, G. Sita Ram, A. Zieger, B. Ziegler: *Nucl. Phys. A* **251** (1975) 479

[39] F. E. Bertrand, R. W. Peelle: *Phys. Rev. C* **8** (1973) 1045

[40] M.B. Chadwick, P.G. Young, S. Chiba: *Journal of Nucl. Sci. and Tech.* (1995, *to be published*)